Synthesis, Molecular Structure, Crystal Packing, and Dynamic Behaviour in the Solid State of $[Fe_2(\eta^5-C_5H_5)_2(\mu-CO)(CO)_2\{\mu-CR(CN)\}]$ (R = H or CN)†

Silvio Aime,*[a] Lucia Cordero,[a] Roberto Gobetto,[a] Silvia Bordoni,[b] Luigi Busetto,*[b] Valerio Zanotti,[b] Vincenzo G. Albano,[c] Dario Braga*[c] and Fabrizia Grepioni[c]

[a] *Dipartimento di Chimica Inorganica, Chimica Fisica e Chimica dei Materiali, University of Torino, Via P. Giuria 7, 10125, Torino, Italy*

[b] *Dipartimento di Chimica Fisica ed Inorganica, University of Bologna, Via Risorgimento 8, 40136 Bologna, Italy*

[c] *Dipartimento di Chimica 'G. Ciamician', University of Bologna, Via F. Selmi 2, 40126 Bologna, Italy*

The dinuclear complexes $[Fe_2(\eta^5-C_5H_5)_2(\mu-CO)(CO)_2\{\mu-CH(CN)\}]$ **1** and $[Fe_2(\eta^5-C_5H_5)_2(\mu-CO)(CO)_2\{\mu-C(CN)_2\}]$ **2** have been obtained from the sulfonium cation $[Fe_2(\eta^5-C_5H_5)_2(\mu-CO)(CO)_2\{\mu-C(SMe_2)(CN)\}]^+$ *via* SMe_2 displacement with H^- and CN^-, respectively. Complex **1** is present in solution and in the solid state as a mixture of isomers, the relative composition depending on the solvent. The structures of the *cis* isomers of **1** (*cis*-**1a**) and **2** (*cis*-**2**) have been determined by single-crystal X-ray diffraction: *cis*-**1a**, monoclinic, space group $P2_1/m$, $a = 6.408(1)$, $b = 13.58(1)$, $c = 8.004(1)$ Å, $\beta = 93.17(2)°$, $Z = 2$, 2225 measured, 1392 unique observed reflections $[I > 2.0\sigma(I)]$, $R = 0.035$, $R' = 0.036$; *cis*-**2**, orthorhombic, space group *Pnma*, $a = 10.346(3)$, $b = 12.313(4)$, $c = 12.590(3)$ Å, $Z = 4$, 1645 measured, 1115 unique observed reflections $[I > 2.0\sigma(I)]$, $R = 0.027$, $R' = 0.029$. The dynamic behaviour of the two complexes in the solid state has been investigated by variable-temperature ^1H spin–lattice relaxation time measurements and ^{13}C magic angle spinning NMR spectroscopy. The activation energies for the reorientational processes have been estimated. The separate intra- and inter-molecular contributions to the total reorientational barriers have been evaluated by means of potential-energy barrier calculations within the pairwise atom–atom approach.

The rotational motion of C_5H_5 rings about their co-ordination axes in crystals of several metallocenes was suggested many years ago by Anderson[1] on the basis of the temperature dependence of the ^1H NMR second moment. Afterwards, several papers[2] dealt with the determination of the activation energies associated with ring reorientation of π-bonded cyclic ligands in organometallic compounds by using ^1H NMR measurements of the spin–lattice relaxation time T_1, this latter technique allowing the exploitation of a wider temperature range with respect to second-moment measurements. Insights into the nature of the dynamic processes and an estimate of the energy barrier opposing ring reorientation can also be obtained by means of atom–atom potential-energy calculations if information on the molecular and crystal structure is available.[3] In most cases the combined use of spectroscopic and crystallographic methods has proved essential to understanding of the solid-state dynamic behaviour shown by molecules or molecular fragments in organometallic crystals.[4] For instance, the reorientational motion of the two structurally independent C_5H_5 rings in the *cis* isomer of $[Fe_2(\eta^5-C_5H_5)_2(\mu-CO)_2(CO)_2]$ has been investigated by ^1H spin–lattice relaxation-time measurements showing that the two rings reorientate with two different activation energies in the solid state.[5a] These differences could also be evaluated by computing the potential barriers to ring jumps and by comparing the extent of librational motion of the two rings about equilibrium positions as evidenced by the atomic anisotropic displacement parameters.[5b] The dynamic processes occurring in crystalline organometallic materials containing substituted benzene or cyclopentadienyl ligands have also recently been investigated by a combined use of solid-state NMR techniques and empirical calculations.[6]

In this paper we apply these methods jointly to investigate the solid-state dynamic behaviour of $[Fe_2(\eta^5-C_5H_5)_2(CO)_3\{CH(CN)\}]$ **1** and $[Fe_2(\eta^5-C_5H_5)_2(CO)_3\{C(CN)_2\}]$ **2**. This work is aimed at an assessment of the role of remote substitution on the reorientational rates of the C_5H_5 ligands with respect to the parent carbonyl complex $[Fe_2(\eta^5-C_5H_5)_2(\mu-CO)_2(CO)_2]$.

The molecular and crystal structures of these two novel species have been determined by single-crystal X-ray diffraction. The main difference at the molecular level between these molecules and that of *cis*-$[Fe_2(\eta^5-C_5H_5)_2(\mu-CO)_2(CO)_2]$ arises from the substitution of a CH(CN) in **1** and of a $C(CN)_2$ group in **2** for a bridging CO group in the latter molecule. The solution NMR and IR spectra were indicative of the presence of three isomers in the case of complex **1**, whereas **2** appears to be present as a single isomeric form. We will proceed first by discussing the synthesis of the two species and their molecular and crystal structures, and then by illustrating the solid-state NMR experimental findings in comparison with the results of potential-energy calculations.

Results and Discussion

Synthesis and Chemical Characterization.—The dicyanocarbene complex **2** was first synthesised by King and Saran[7] in very low yield (6%) by treating the carbonylate anion $[Fe_2(\eta^5-C_5H_5)_2(CO)_2]^-$ with $(NC)_2CBr_2$. We have recently demonstrated[8] that the sulfonium salt $[Fe_2(\eta^5-C_5H_5)_2(\mu-CO)(CO)_2\{\mu-C(SMe_2)(CN)\}][SO_3CF_3]$ easily undergoes SMe_2 replacement by nucleophiles providing an excellent entry into the

† *Supplementary data available:* see Instructions for Authors, *J. Chem. Soc., Dalton Trans.*, 1992, Issue 1, pp. xx–xxv.

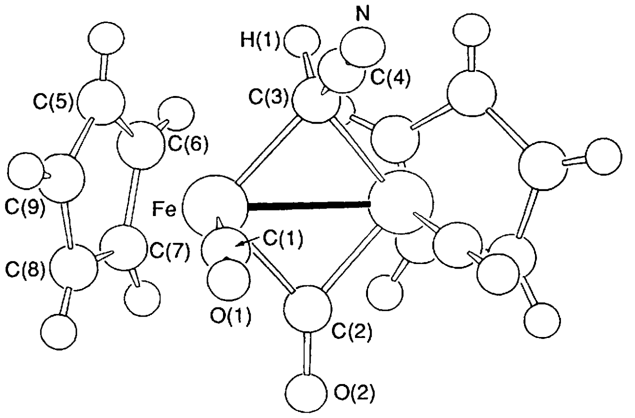

Fig. 1 The molecular structure of complex *cis*-**1a** showing the atomic labelling scheme

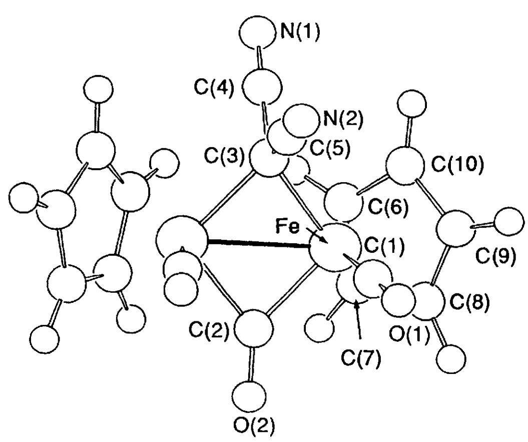

Fig. 2 The molecular structure of complex *cis*-**2** showing the atomic labelling scheme

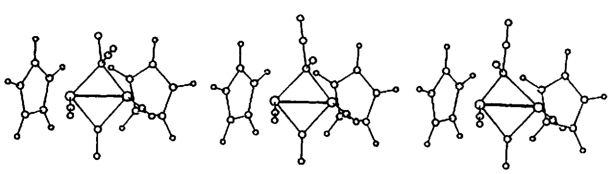

chemistry of the iron dinuclear μ-cyanocarbene complexes including **1** and **2**. Compound **1** has been shown to exist in solution as a mixture of the three isomers shown. These isomers, in spite of our efforts, could not be separated by column chromatography on alumina gel or fractional crystallization.

The isomer ratio in CD_2Cl_2 solution was estimated from ^1H and ^{13}C NMR spectroscopy. The resonances of the methylidene proton (δ 8.86, *cis*-**1b**; 7.94, *trans*-**1**; 6.81, *cis*-**1a**) were attributed by analogy with the related complexes [$Fe_2(\eta^5$-$C_5H_5)_2$(μ-CO)-$(CO)_2${μ-CH(SR)}][9a] for which the lowest-field ^1H NMR methylidene proton signal was assigned to the *cis* isomer bearing H on the C_5H_5 side. Moreover only the *trans* isomer is expected to give rise to two, equally intense, C_5H_5 signals (at δ 92.2 and 90.2 in the ^{13}C NMR spectrum) allowing the attribution of the remaining C_5H_5 resonances to the *cis* isomer.

The relative abundance of the *cis* and *trans* isomers for complex **1** varies with solvent polarity, the *cis* configuration being favoured in polar solvents. For example, the 3.3:1.6:1 *cis*-**1a**:*cis*-**1b**:*trans*-**1** ratio in CD_2Cl_2 becomes 3.0:6.5:1 in CD_3CN. Such a composition was attained within a few minutes of preparing the solution and did not vary with time. These results suggest the existence of a rapid *cis–trans* equilibrium as reported for the related complexes [$Fe_2(\eta^5$-$C_5H_5)_2$(μ-CO)-$(CO)_2${μ-C(SR)(SR′)}][9a] and [$Fe_2(\eta^5$-$C_5H_5)_2$(μ-CO)$(CO)_2$-{μ-C(CMe$_2$)}].[9b]

Table 1 Relevant bond distances (Å) and angles (°) for complexes *cis*-**1a** and *cis*-**2**

	cis-**1a**		*cis*-**2**
Fe–Fe′	2.529(1)	Fe–Fe′	2.538(1)
Fe–C(1)	1.756(3)	Fe–C(1)	1.776(3)
C(1)–O(1)	1.140(4)	C(1)–O(1)	1.143(3)
Fe–C(2)	1.917(3)	Fe–C(2)	1.930(3)
C(2)–O(2)	1.172(5)	C(2)–O(2)	1.173(5)
Fe–C(3)	1.976(3)	Fe–C(3)	1.997(2)
C(3)–C(4)	1.428(5)	C(3)–C(4)	1.439(5)
C(4)–N	1.146(6)	C(4)–N(1)	1.151(4)
C(3)–H(1)	1.06(2)	C(3)–C(5)	1.448(4)
		C(5)–N(2)	1.155(4)
Fe–C(5)	2.123(3)	Fe–C(6)	2.109(3)
Fe–C(6)	2.138(3)	Fe–C(7)	2.114(3)
Fe–C(7)	2.127(3)	Fe–C(8)	2.091(4)
Fe–C(8)	2.102(3)	Fe–C(9)	2.074(4)
Fe–C(9)	2.091(3)	Fe–C(10)	2.115(3)
C(5)–C(6)	1.401(5)	C(6)–C(7)	1.375(5)
C(6)–C(7)	1.399(5)	C(7)–C(8)	1.414(6)
C(7)–C(8)	1.409(5)	C(8)–C(9)	1.384(8)
C(8)–C(9)	1.405(5)	C(9)–C(10)	1.367(6)
C(5)–C(9)	1.403(5)	C(6)–C(10)	1.372(5)
Fe–C(1)–O(1)	177.1(3)	Fe–C(1)–O(1)	178.7(2)
Fe–C(2)–O(2)	138.7(1)	Fe–C(2)–O(2)	138.9(1)
H(1)–C(3)–C(4)	110(3)	C(4)–C(3)–C(5)	107.9(3)
C(3)–C(4)–N	179.4(6)	C(3)–C(4)–N(1)	179.5(3)
		C(3)–C(5)–N(2)	179.8(3)

Crystallization of complex **1** from a CH_2Cl_2 solution layered with hexane afforded a red precipitate from which crystals suitable for X-ray diffraction were recovered.

Complex **2** exists in solution as a mixture of *cis* and *trans* isomers though the *cis* isomer has been found to be, by far, the most abundant (*cis*:*trans* ratio *ca.* 10:1 evaluated from ^{13}C NMR spectra in CD_3NO_2). The structure of compound *cis*-**2** has also been determined by X-ray diffraction as described below.

The Molecular and Crystal Structures of Isomers cis-**1a** *and cis*-**2**.—The molecular structures of *cis*-**1a** and *cis*-**2** as determined in the solid state are closely related and will be described together. Relevant structural parameters are listed in Table 1, and molecular diagrams and labelling schemes are shown in Figs. 1 and 2 for *cis*-**1a** and *cis*-**2**, respectively. Both molecules possess the familiar double-bridged Fe–Fe system common to most carbene derivatives of [$Fe_2(\eta^5$-$C_5H_5)_2$(μ-CO)$_2$(CO)$_2$].[10] The two cyclopentadienyl ligands adopt a *cis* conformation. Both molecules possess crystallographic *m* symmetry with the mirror plane bisecting the Fe–Fe bond and comprising the bridging carbene unit and the bridging CO ligand.

The C–C≡N groups have strictly comparable geometries in isomers *cis*-**1a** and *cis*-**2**: they are linear [C–C–N 179.4(6) in *cis*-**1a**, 179.5(3) and 179.8(3)° in *cis*-**2**] and show similar values of the C–C and C≡N distances [C–C 1.428(5) in *cis*-**1a** 1.439(5) and 1.448(4) Å in **2**; C≡N 1.146(6) in *cis*-**1a** 1.151(4) and 1.155(4) Å in *cis*-**2**]. Interestingly, the H–C–(CN) and the (NC)–C–(CN) angles in the two complexes are close to an ideal sp^3 value [110(3) in *cis*-**1a**, 107.9(3)° in *cis*-**2**].

In terms of molecular shape the two complexes differ essentially in the substitution of the H atom bound to the C(carbene) atom in *cis*-**1a** for the second CN group in *cis*-**2**. This is a small difference which has a dramatic effect on the whole pattern of intermolecular interactions in the crystal and, consequently, on the dynamic behaviour of the two species in the solid state (see next section).

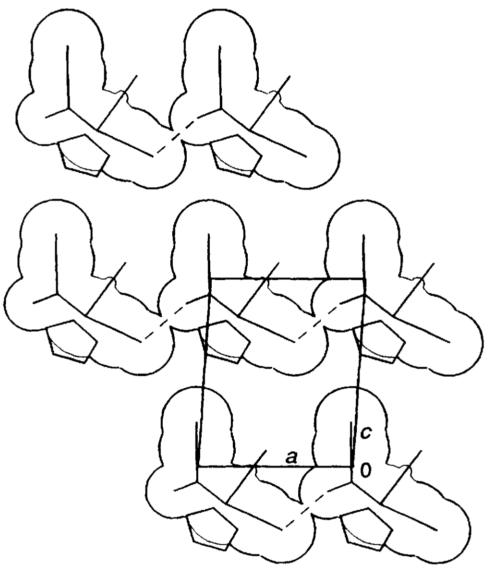

Fig. 3 Projections of the molecular distribution in crystalline complex *cis*-**1a** along the 010 direction. The space-filling outlines mark the atomic groups bisected by the crystallographic mirror plane. Note how the space-filling atomic spheres of the H(carbene) and CO groups intersect indicating the presence of intermolecular hydrogen-bonding interactions

Both crystals can be regarded as constituted of a stacking sequence of layers in which the molecules are placed parallel to each other with the Fe–Fe bonds bisected by the crystallographic mirror planes, which contain the HC(CN) and (NC)C(CN) groups of atoms (as well as the bridging CO groups). In *cis*-**1a** the packing distribution allows close proximity between the C(carbene)-H groups and the bridging CO ligands of neighbouring molecules, thus establishing a network of weak hydrogen-bonding interactions [O ··· H 2.51(2) Å, O ··· H–C 160°] (see Fig. 3), which are, obviously, not present in crystalline *cis*-**2**. As a consequence, the molecular packing is tighter in *cis*-**1a** than in *cis*-**2**. This is reflected in the values of Kitaigorodsky's packing coefficients[14b] (0.56 *vs.* 0.53), and in a conspicuous difference between the values of the packing potential energy computed for the two complexes (−210 *vs.* −170 kJ mol^{-1}).

The difference in packing efficiency is also reflected in the different extent of intermolecular control on the reorientational motion of the C_5H_5 ligands in the two complexes as discussed in the following sections.

^{13}*C Cross Polarization Magic Angle Spinning (CP MAS) Spectra of Complexes* **1** *and* **2**.—Compound **1** as a bulk solid shows a number of resonances in the ^{13}C CP MAS NMR spectrum which is consistent only with the presence of a mixture of different isomeric species. Particularly interesting is the isotropic region corresponding to the bridging carbonyls which shows three resonances at δ 264.3, 266.8 and 271.6 in the relative intensity ratio of 5:1:4. Since there is only one μ-bridging CO per molecule we may interpret the observed pattern on the basis of the three (*cis*-**1a**, *cis*-**1b**, *trans*-**1**) isomers.

The observation of two C_5H_5 ^{13}C resonances of similar intensity at δ 91.7 and 90.1, respectively, has to be attributed to crystallographically equivalent pairs of rapidly reorientating C_5H_5 groups of the two main isomers. On the assumption that the relative position of the chemical shifts found in solution is maintained in the solid state, the two peaks can be tentatively assigned to *cis*-**1a** and *cis*-**1b**, respectively. Accordingly, the low-intensity resonances due to the minor component *trans*-**1** are clearly masked by the strong absorptions due to *cis*-**1a** and *cis*-**1b**. Support for the assignment of *trans*-**1** as the minor component comes from the observation that, if *trans*-**1** were one of the two principal species, a strongly asymmetric doublet pattern (arising from the overlap of the single resonance due to *trans*-**1** with that of the other isomer present in similar amount) should be seen in the C_5H_5 region of the solid-state spectrum.

The ^{13}C resonances of the cyano-groups behave similarly to those of the bridging ^{13}CO, whereas the terminal carbonyls of the different isomers give rise to a single, slightly broadened absorption at δ 213.

The spectral pattern shown in the ^{13}C CP MAS NMR spectrum of complex **1** clearly indicates that the three isomeric forms detected in solution are maintained in the solid state. Samples of compound **1** obtained from different solvent mixtures showed marked changes in the distribution of the three isomers. Sublimation too seems markedly to affect the isomer ratio. Interestingly, the same ^{13}C CP MAS spectral pattern was observed for the sample from which crystals used for the X-ray diffraction experiment had been selected.

The ^{13}C CP MAS NMR spectrum of complex **2** shows the presence of a single species with a μ-CO at δ 258, two equivalent terminal CO groups at δ 210, two different CN groups at δ 130 and 133 respectively, two equivalent C_5H_5 ligands at δ 92 and a μ-C resonance at δ 59. For compound **2** we have also been able to calculate the CN group chemical shift anisotropy (CSA): we have obtained a value of 288.7 ppm with tensor components σ_{11} = 262.9, σ_{22} = 195.6 and σ_{33} = 59.5 ppm.

For the intense C_5H_5 ^{13}C signals of both complexes **1** and **2**, T_1 measurements were carried out by using the pulse sequence proposed by Torchia,[11] which allows the determination of the longitudinal relaxation time of the ^{13}C nuclei under cross polarization conditions. Quite different values of the relaxation times were obtained: 12.4 and 8.6 s for the two C_5H_5 resonances of the spectrum of compound **1** (assigned to *cis*-**1a** and *cis*-**1b**, respectively), whereas a value of 25.5 s was found for **2**. These results clearly indicate that the C_5H_5 rings are rotating (at ambient temperature) at different rates; quantitative determination of the activation energy of these motions has been achieved by wide-line ^{1}H relaxation time measurements at different temperatures.

T_1 ^{1}H *NMR Profiles*.—The longitudinal proton relaxation times of solid complexes **1** and **2** were measured in the temperature range 378–163 K and the resulting profiles are in Fig. 4(*a*) and (*b*). The profile obtained for **1** looks rather complicated since it results from the contribution of three isomeric species (very likely corresponding to four different C_5H_5 resonances) in the ratio determined from the ^{13}C CP MAS spectrum. Although the profile is in general rather flat, three minima may be recognized at 283, 208 and 169 K, respectively. Taking these T_1 minima as the points at which the modulation of the C–H interaction is more efficient ($\omega\tau_c$ = 0.62, where ω is the Larmor frequency and τ_c is the correlation time), we computed the T_1 profiles corresponding to the rotation of three different C_5H_5 ligands. The sum of the three contributions weighted according to the relative ratios found for *cis*-**1a**, *cis*-**1b** and *trans*-**1** in the ^{13}C CP MAS spectrum agrees quite well with the observed profile.

As previously shown[12] the individual profiles of log T_1 *vs.* $1000/T$ afford the activation energy (E_A) associated with the reorientational process; the E_A values in this case were 16.0, 13.1 and 11.5 kJ mol^{-1}. The assignment of the process characterized by E_A 16.0 kJ mol^{-1} to the isomer *trans*-**1** is made on the basis of its minor intensity in the $1/T_1$ *vs.* $1000/T$ profile. The assignment of the two lower activation energies to *cis*-**1a** and *cis*-**1b**, respectively, has been possible on the basis of the differences found in T_1 ^{13}C CP MAS spectra. At ambient temperature, we are in the extreme-narrowing limit where $1/T_1$ (for ^{13}C) $\propto \tau_c$. This implies that the ^{13}C resonance with the shorter T_1 (*cis*-**1a**) has to be related to the proton T_1 profile which shows a minimum at 208 K and an E_A value of 13.1 kJ mol^{-1}.

The profile of proton longitudinal relaxation times *vs.* $1000/T$ for solid complex **2** is almost a straight line the slope of which

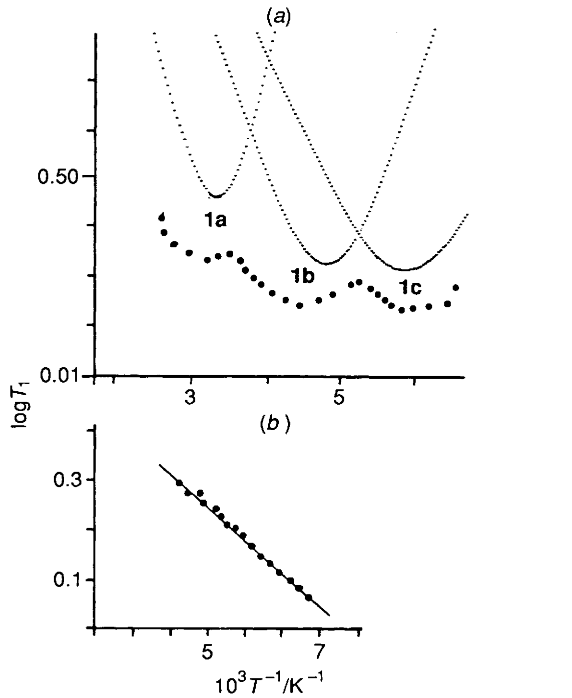

Fig. 4 Variation of proton spin-lattice relaxation times T_1 with inverse temperature T^{-1} for crystalline complexes **1** (*a*) and **2** (*b*) at 270 MHz

affords an E_A as low as 4 kJ mol^{-1}. A low activation energy for this process could be predicted on the basis of the quite long ^{13}C relaxation time. In summary, ^1H wide-line experiments and ^{13}C high-resolution spectra indicate that the C_5H_5 rings rotate more easily in **2** than in each of the isomers **1**.

In order to gain insight into the causes of this behaviour we resorted to the investigation of the dynamic processes by means of atom–atom potential-energy barrier (AAPEB) calculations.[4]

C_5H_5 *Reorientation in Isomers cis-***1a** *and cis-***2** *from AAPEB Calculations.*—In both crystalline isomers *cis*-**1a** and *cis*-**2** the two C_5H_5 ligands are related by the mirror planes bisecting the Fe–Fe bonds, so that there is only one (symmetry-independent) reorientational process to be estimated. As previously discussed,[3,4] AAPEB calculations allow a discrimination between inter- and intra-molecular non-bonding contributions to the reorientational potential-energy barrier (PB hereafter). It is worth stressing that this kind of discrimination, though rather qualitative, is not possible with other methods. The NMR activation energy, in particular, is obtained as a mean value measured over a range of temperatures and convolutes all possible *internal* contributions (arising from bonding and non-bonding intramolecular interactions) to the energy barrier.[4] In most cases of C_5H_5 reorientation, however, the intramolecular terms are null or negligible {this is the case for all metallocene species, but also for the *cis* and *trans* isomers of $[Fe_2(\eta^5\text{-}C_5H_5)_2(CO)_4]$}.[5b]

In crystalline isomer *cis*-**1a** at the equilibrium position (0° rotation of the C_5H_5 ligand) PB_{inter} is at a minimum and increases rapidly on both sides of the potential well as the ligand is rotated around an axis passing through its centre of mass and the co-ordinated Fe atom; PB_{inter} shows the usual sinusoidal profile with equivalent minima every $2\pi/5$ rotational jumps, and maxima not exceeding 28.7 kJ mol^{-1}. The value of PB_{intra} at the equilibrium position (5.0 kJ mol^{-1}), on the contrary, is somewhat 'midway' between a minimum (corresponding to a $-20°$ rotation of the ligand from equilibrium) and a maximum (at $+10°$ from equilibrium). The PB_{inter} and PB_{intra} are, therefore, not in phase, resulting in a PB_{tot} barrier of 27.2 kJ mol^{-1}.

The situation is rather different in crystalline isomer *cis*-**2**: the looser crystal packing is reflected in a substantial decrease in the value of PB_{inter} with respect to crystalline *cis*-**1a** [*ca.* 6.3 kJ mol^{-1}]; the presence of the more sterically demanding CN group with respect to the H atom causes, on the other hand, a substantial increase in PB_{intra} (11.7 kJ mol^{-1}). It is clear that in *cis*-**2** the intramolecular repulsions are dominating the conformational choice, so that it is not surprising that the intramolecular potential-energy profile has a minimum at 0° rotation as well as every 72° rotational displacement, while the PB_{inter} profile shows minima after a -30 or $+40°$ rotation from the equilibrium position. The two contributions sum to give a PB_{tot} of 7.9 kJ mol^{-1}.

On the basis of these observations it seems possible to conclude that the (experimentally observed) orientation of the C_5H_5 ligands in isomer *cis*-**1a** is determined essentially at the intermolecular level, while in *cis*-**2** it is determined at the intramolecular level. This is in agreement with the observation that crystal cohesion [in terms of computed packing potential energy (PPE)] in *cis*-**2** is *ca.* 20% less than in *cis*-**1a**, *i.e.* in *cis*-**2** optimization of the intramolecular potential appears to occur at the expense of the packing cohesion. As far as C_5H_5 reorientation is concerned, although the ratio between the values of PB_{tot} in *cis*-**1a** and *cis*-**2** reproduces that between the activation energies well, the actual reorientational barriers are slightly higher than the activation energies obtained from the spectroscopic experiments. This difference arises from the 'static environment' approximation that is known to cause overestimation of the intermolecular repulsions in AAPEB calculations.[4]

Experimental

Syntheses of Complexes **1** *and* **2**.—All reactions were routinely carried out under nitrogen by standard Schlenk techniques. Solvents were distilled immediately before use under nitrogen from appropriate drying agents. Instruments employed: IR, Perkin Elmer 983-G; NMR, Varian Gemini 200. Elemental analyses were by Pascher Microanalytical Laboratory (Remagen, Germany). Compounds **1** and $[Fe_2(\eta^5\text{-}C_5H_5)_2(\mu\text{-}CO)(CO)_2\{\mu\text{-}C(SMe_2)(CN)\}][SO_3CF_3]$ were prepared according to published methods.[8a–c]

$[Fe_2(\eta^5\text{-}C_5H_5)_2(\mu\text{-}CO)(CO)_2\{\mu\text{-}C(CN)_2\}]$ **2**. To a stirred solution of $[Fe_2(\eta^5\text{-}C_5H_5)_2(\mu\text{-}CO)(CO)_2\{\mu\text{-}C(SMe_2)(CN)\}][SO_3CF_3]$ (0.37 g, 0.64 mmol) in MeCN (10 cm^3) was added $NBu^t{}_4CN$ (0.19 g, 0.70 mmol). The mixture was stirred for 15 min and the solvent removed *in vacuo*. The residue was dissolved in dichloromethane and filtered on an alumina column (3 × 5 cm). The red solution was evaporated to minimum volume, layered with pentane and crystallized at −20 °C to yield 0.20 g (80%) of complex **2** (Found: C, 49.35; H, 2.75. $C_{16}H_{10}Fe_2N_2O_3$ requires C, 49.30; H, 2.60%). IR: $\nu_{max}(CH_2Cl_2)$ 2183w (CN), 2019s, 1989w, 1822m cm^{-1} (CO). NMR: $\delta_H(CD_2Cl_2)$ 5.00 (s, C_5H_5, *cis* + *trans*); $\delta_C(CD_3NO_2)$, *cis*, 255.5 (μ-CO), 205.4 (CO), 125.7, 125.2 (CN) and 87.1 (C_5H_5); *trans*, 204.4 (CO), 88.6 (C_5H_5); *cis*:*trans* = 10:1.

Solid-state ^{13}C *and* ^1H *NMR Measurements.*—High-resolution solid-state ^{13}C NMR spectra were recorded on a JEOL GSE spectrometer using a NM-GSHMU/VT solid-state unit where the ^{13}C nuclei resonate at 67.8 MHz. Samples were contained in rotors (outside diameter 5 mm) in zirconia and spining rates in the range 3.5–4.5 KHz were adjusted to minimize overlap between centre-band and side-band resonances. Chemical shifts (δ scale, high frequency positive) were referenced to external neat liquid tetramethylsilane.

The ^{13}C spin–lattice relaxation times in the solid state were measured by Torchia's method with a proton 90° pulse of 4.5 μs, carbon 90° pulse of 4.5 μs and a contact time of 3.5 ms. Proton spin–lattice relaxation times were measured at 270 MHz by using the inversion recovery pulse sequence (d–180°–τ–90°) where d is the delay time ($d > 5T_1$) and τ is the variable time; the 90° pulse width was 1.5 μs. Typical errors in the evaluation of proton and carbon relaxation times are estimated to be ±2%.

Table 2 Crystal data and details of measurements for complexes *cis*-**1a** and *cis*-**2**

	cis-**1a**	*cis*-**2**
Formula	$C_{15}H_{11}Fe_2NO_3$	$C_{16}H_{10}Fe_2N_2O_3$
M_r	364.96	389.97
Crystal size/mm	0.10 × 0.12 × 0.11	0.14 × 0.12 × 0.15
System	Monoclinic	Orthorhombic
Space group	$P2_1/m$	*Pnma*
a/Å	6.408(1)	10.346(3)
b/Å	13.58(1)	12.313(4)
c/Å	8.004(1)	12.590(3)
β/°	93.17(2)	—
U/Å^3	695.5	1603.8
Z	2	4
F(000)	368	784
μ(Mo-Kα)/cm^{-1}	20.0	17.4
2θ range/°	5–60	5–50
Requested counting σ(*I*)/*I*	0.02	0.01
Prescan rate/° min^{-1}	8	5
Measured reflections	2225	1645
Unique observed reflections [$I > 2.0\sigma(I)$]	1392	1115
No. of refined parameters	123	132
R, R' [b]	0.035, 0.036	0.027, 0.029
S [c]	1.00	1.13
k, g	1.02, 0.002	1.06, 0.0005

[a] Data common to both species: scan mode ω–2θ, ω-scan width 0.7°, prescan acceptance σ(*I*)/*I* = 0.5, maximum scan time = 120 s. [b] $R' = \Sigma[(F_o - F_c)w^{\frac{1}{2}}]/\Sigma F_o w^{\frac{1}{2}}$, where $w = k/[\sigma^2(F) + |g|F^2]$. [c] $S = \{\Sigma_N[w(F_o - F_c)^2]/(N_{obs} - N_{var})\}^{\frac{1}{2}}$.

Table 3 Fractional atomic coordinates for complex *cis*-**1a**

Atom	*x*	*y*	*z*
Fe	0.192 59(5)	0.343 11(2)	0.201 61(4)
C(1)	0.337 2(5)	0.366 2(2)	0.025 7(4)
O(1)	0.433 5(5)	0.384 9(2)	−0.085 6(4)
C(2)	0.402 1(6)	0.25	0.276 7(5)
O(2)	0.570 6(5)	0.25	0.341 5(6)
C(3)	−0.000 7(5)	0.25	0.083 0(4)
C(4)	−0.019 2(8)	0.25	−0.095 6(5)
N	−0.032 1(10)	0.25	−0.238 9(5)
C(5)	−0.057 7(5)	0.435 9(2)	0.264 8(4)
C(6)	0.001 2(5)	0.377 7(2)	0.404 1(4)
C(7)	0.210 1(6)	0.398 8(2)	0.450 4(4)
C(8)	0.282 1(5)	0.469 7(2)	0.338 6(4)
C(9)	0.115 7(6)	0.492 1(2)	0.223 2(4)
H(1)	−0.151(4)	0.25	0.133(6)
H(2)	−0.189(4)	0.433(3)	0.208(5)
H(3)	−0.080(6)	0.330(2)	0.456(5)
H(4)	0.301(5)	0.372(3)	0.535(4)
H(5)	0.423(4)	0.493(3)	0.335(5)
H(6)	0.121(6)	0.540(3)	0.139(4)

Structural Characterization and Crystal Packing Investigation.—The diffraction data for complexes *cis*-**1a** and *cis*-**2** were collected on an Enraf-Nonius CAD-4 diffractometer equipped with a graphite monochromator (Mo-Kα radiation, λ = 0.710 69 Å). Crystal data and details of measurements are summarized in Table 2. The structures were solved by direct methods, which allowed for the location of the Fe atoms, followed by Fourier difference syntheses and subsequent least-squares refinement. Scattering factors for neutral atoms were taken from ref. 13*a*. For all calculations the SHELX 76 program was used.[13b] All atoms, except the H atoms, were treated anisotropically. The H atoms in both species were located directly from final Fourier difference syntheses and refined with 'constraints' on the C–H distances. Common isotropic thermal factors were refined for the $H(C_5H_5)$ in both species [0.066(5), 0.110(7) Å in *cis*-**1a** and *cis*-**2**, respectively]. Fractional atomic coordinates are in Tables 3 and 4, respectively.

Table 4 Fractional atomic coordinates for complex *cis*-**2**

Atom	*x*	*y*	*z*
Fe	0.217 98(2)	0.127 35(3)	0.565 51(3)
C(1)	0.126 0(2)	0.096 9(3)	0.459 8(2)
C(2)	0.289 9(3)	0.25	0.473 9(4)
C(3)	0.116 7(2)	0.25	0.637 6(2)
C(4)	0.116 8(3)	0.25	0.751 8(3)
C(5)	0.004 8(2)	0.25	0.602 2(2)
N(1)	0.116 0(3)	0.25	0.843 2(2)
N(2)	−0.084 3(2)	0.25	0.573 8(2)
O(1)	0.067 9(2)	0.075 2(2)	0.391 2(2)
O(2)	0.349 6(3)	0.25	0.401 4(3)
C(6)	0.311 2(3)	0.075 4(3)	0.699 4(3)
C(7)	0.374 4(3)	0.062 7(4)	0.610 0(4)
C(8)	0.322 4(5)	−0.030 0(5)	0.544 9(3)
C(9)	0.229 5(4)	−0.068 7(3)	0.597 9(5)
C(10)	0.223 2(3)	−0.005 5(3)	0.693 1(3)

Additional material available from the Cambridge Crystallographic Data Centre comprises H-atom coordinates, thermal parameters and remaining bond lengths and angles.

The molecular environment in the crystal lattice of complexes *cis*-**1a** and *cis*-**2** has been investigated by means of the expression $PPE = \Sigma_i\Sigma_j[A\exp(-Br_{ij}) - Cr_{ij}^{-6}]$, where PPE represents the packing potential energy[14a] and r_{ij} the non-bonded atom–atom intermolecular distance. Index *i* in the summation runs over all atoms of one molecule (chosen as reference molecule) and *j* over the atoms of the surrounding molecules distributed according to crystal symmetry. A cut-off of 10 Å was adopted. The values of coefficients *A*–*C* used were taken from ref. 14*b* and are discussed in previous papers. The results of the PPE calculations were used to select the first-neighbouring molecules among those surrounding the one chosen as reference on the basis of the contribution to the PPE. The values of the reorientational barriers were obtained by recalculating the PPE at various rotational steps during C_5H_5 reorientation, and by subtracting the PPE corresponding to the observed structure. These calculations were carried out in a non-co-operating environment ('static environment' approximation) but with allowance for a separate estimate of the intra- and inter-molecular contributions. All calculations were carried out with the aid of the computer program OPEC;[15] SCHAKAL 88[16] was used for the graphical representation of the results.

Acknowledgements

We thank Dr. Guy Orpen for useful discussions and comments. Financial support by Ministero dell' Universita' e della Ricerca Scientifica e Tecnologica and by Consiglio Nazionale delle Ricerche is acknowledged.

References

1 S. Anderson, *J. Organomet. Chem.*, 1974, **71**, 263
2 I. S. Butler, P. J. Fitzpatrick, D. F. R. Gilson, G. Gomez and A. Shaver, *Mol. Cryst. Liq. Cryst.*, 1981, 71; C. H. Holm and J. A. Ibers, *J. Chem. Phys.*, 1959, **30**, 885; D. F. R. Gilson and G. Gomez, *J. Organomet. Chem.*, 1982, **240**, 41.
3 D. Braga and F. Grepioni, *Organometallics*, 1992, **11**, 717.
4 D. Braga, *Chem. Rev.*, 1992, **92**, 633.
5 (*a*) S. Aime, M. Botta, R. Gobetto and A. Orlandi, *Magn. Reson. Chem.*, 1990, **28**, S52; (*b*) D. Braga, C. Gradella and F. Grepioni, *J. Chem. Soc., Dalton Trans.*, 1989, 1721.
6 S. Aime, D. Braga, R. Gobetto, F. Grepioni and A. Orlandi, *Inorg. Chem.*, 1991, **30**, 951; S. Aime, D. Braga, L. Cordero, R. Gobetto, F. Grepioni, S. Righi and S. Sostero, *Inorg. Chem.*, 1992, **31**, 3054.
7 R. B. King and M. S. Saran, *J. Am. Chem. Soc.*, 1973, **95**, 1811.
8 (*a*) V. G. Albano, S. Bordoni, D. Braga, L. Busetto, A. Palazzi and V. Zanotti, *Angew. Chem., Int. Ed. Engl.*, 1991, **30**, 847; (*b*) L. Busetto,

M. C. Cassani, V. Zanotti, V. G. Albano and D. Braga, *J. Organomet. Chem.*, 1991, **415**, 395; (*c*) L. Busetto, V. Zanotti, S. Bordoni, L. Carlucci, V. G. Albano and D. Braga, *J. Chem. Soc., Dalton Trans.*, 1992, 1105.

9 (*a*) N. C. Schroeder, R. Funchess, R. A. Jacobson and R. J. Angelici, *Organometallics*, 1989, **8**, 521; (*b*) A. F. Dyke, S. A. R. Knox, M. J. Morris and P. Naish, *J. Chem. Soc., Dalton Trans.*, 1983, 1417.

10 R. F. Brian, P. T. Greene, M. J. Newlands and D. J. Field, *J. Chem. Soc A*, 1970, 3068.

11 D. A. Torchia, *J. Magn. Reson.*, 1978, **30**, 613.

12 Z. Navankiewicz, A. L. Blumenfeld, V. L. Bondaneva, I. A. Mamedyarova, M. N. Nefedova and V. I. Sokolov, *J. Incl. Phenom. Mol. Recogn. Chem.*, 1991, **11**, 233.

13 (*a*) *International Tables for X-Ray Crystallography*, Kynoch Press, Birmingham, 1975, vol. 4, pp. 99–149; (*b*) G. M. Sheldrick, SHELX 76, Program for Crystal Structure Determination, University of Cambridge, 1976.

14 (*a*) A. J. Pertsin and A. I. Kitaigorodsky, *The Atom–Atom Potential Method*, Springer, Berlin, 1987; (*b*) A. I. Kitaigorodsky, *Chem. Soc. Rev.*, 1978, **7**, 133; (*c*) K. Mirsky, *Computing in Crystallography, Proceedings of the International Summer School on Crystallographic Computing*, Delft University Press, Twente, 1978, 169; (*d*) A. Gavezzotti and M. Simonetta, *Chem. Rev.*, 1982, **82**, 1.

15 A. Gavezzotti, OPEC, Organic Packing Potential Energy Calculations, University of Milano; see also, *J. Am. Chem. Soc.*, 1983, **105**, 5220.

16 E. Keller, SCHAKAL 88, Graphical Representation of Molecular Models, University of Freiburg, 1988.

Received 12th May 1992; Paper 2/02460H